Spectral functions for strongly correlated 5*f* electrons

F. Pollmann and G. Zwicknagl
Institut fur Mathematische Physik, Technische Universitt Braunschweig, Mendelsohnstrasse 3, 38106 Braunschweig, Germany
(Received 7 September 2005; revised manuscript received 23 November 2005; published 23 January 2006)

We calculate the spectral functions of model systems describing 5*f* compounds adopting cluster perturbation theory. The method allows for an accurate treatment of the short-range correlations. The calculated excitation spectra exhibit coherent 5*f* bands coexisting with features associated with local intra-atomic transitions. The findings provide a microscopic basis for partial localization. Results are presented for linear chains.

DOI: 10.1103/PhysRevB.73.035121 PACS number(s): 71.10.−w, 71.27.+a, 79.60.−i

I. INTRODUCTION

Electronic correlations are strongly evident in actinide intermetallic compounds. The highly complex phase diagrams with novel sometimes enigmatic ordered states reflect a sensitivity to small changes in external control parameters like temperature, pressure, and magnetic fields.[1] An undispensible prerequisite for an explanation of the observed anomalies is a microscopic understanding of the strongly interacting 5*f* electrons which partially preserve atomiclike character. Occupying the partially filled 5*f* shells according to Hund's rules leads to magnetic moments. The lifting of rotational symmetry in a crystal by the crystalline electric field (CEF) and the hybridization with the delocalized conduction states of the outer-shell electrons leads to a large number of low-energy excitations.

Of particular interest are the heavy-fermion phases where the low-energy excitations correspond to heavy quasiparticles. Their enhanced effective masses m^* are reflected in enhanced values of the Sommerfeld coefficient and the Pauli spin susceptibility. The heavy quasiparticles have been observed by de Haas–van Alphen (dH-vA) experiments in a number of compounds. The experiments unambiguously confirm that some of the U 5*f* electrons must have itinerant character. It has been known for quite some time that the 5*f* states in actinide intermetallic compounds cannot be considered as ordinary band states. Standard band-structure calculations based on the local density approximation (LDA) fail to reproduce the narrow quasiparticle bands. On the other hand, the predicted bandwidths are too small to explain photoemission data.[2,3] These shortcomings are a direct consequence of the inadequate treatment of local correlations within ordinary electron-structure calculations.

Increasing experimental evidence points towards a two-fluid model implying the co-existence of both localized atomiclike and itinerant bandlike 5*f* states. For U heavy-fermion compounds the photoemission spectra usually display a two-peaked structure in the 5*f* emission.[4,5] The peak at 1 eV binding energy results from the localized 5*f* states while the narrow peak at the Fermi level is attributed to 5*f*-derived itinerant quasiparticles.[6] Concerning the low-energy excitations it has been shown recently that the dual model allows for a quantitative description of the renormalized quasiparticles—the heavy fermions—in UPd_2Al_3. The measured dH-vA frequencies for the heavy-quasiparticle portions as well as the large anisotropic effective masses can be explained very well by treating two of the 5*f* electrons as localized.[7,8] Finally, the coexistence of 5*f*-derived quasiparticles and local magnetic excitations in this compounds has been confirmed by recent neutron scattering experiments.[9] Theoretical studies aimed at an explanation of the complex low-temperature structures lay emphasis on the partitioning of the electronic density into localized and delocalized parts.[10,11] Considering the success of the dual model in describing the low-energy behavior of actinide heavy-fermion compounds we have to explain how the splitting of the 5*f* shells arises and propose means of identifying the underlying microscopic mechanism.

The dual model as sketched above is an effective Hamiltonian for the low-energy regime. In the spirit of Wilson's renormalization group it should be obtained by integrating out processes at higher energies. The central theoretical task is to identify the microscopic mechanisms which cause the 5*f*-band widths to renormalize to almost zero for certain orbital symmetries while staying finite for others. In the present paper we concentrate on the role of intra-atomic correlations, the motivation being as follows: Recent model studies for the ground-state properties of small clusters show that intra-atomic correlations as described by Hund's rules may strongly enhance anisotropies in the kinetic energy and thus lead to an orbital-selective Mott transition in 5*f* systems.[8,12] This scenario closely parallels the one postulated recently to explain the behavior of transition-metal oxides.[13–16] Here we discuss how intra-atomic correlations affect the single-particle spectral functions. The conjecture is that the above-mentioned enhancement of anisotropies in the kinetic energy can explain the dual nature of the 5*f* electrons. In a real material this enhancement would imply anisotropies far beyond these predicted by a standard electronic-structure calculation.

The concept of correlation-driven partial localization in U compounds has been challenged by various authors (see, e.g., Ref. 17). The conclusions are drawn from the fact that conventional band-structure calculations within the LDA which treat all 5*f* states as itinerant can reproduce ground-state properties like Fermi-surface topologies and densities. The calculation of ground-state properties, however, cannot provide conclusive evidence for the delocalized or localized character of the 5*f* states in actinides. First, the presence of localized states can be simulated in standard band calculations by filled bands lying (sufficiently far) below the Fermi level. Second, the Fermi surface is mainly determined by the

number of particles in partially filled bands and the geometry of the lattice which affects the dispersion of the conduction electrons. A change in the number of band electrons by an even amount does not necessarily affect the Fermi surface since a change by an even number may correspond to adding or removing a filled band. As such, the Fermi surface is not a sensitive test of the microscopic character of the states involved.

Following up this track of thought we would like to present here a qualitative discussion of strongly correlated $5f$ systems, emphasizing properties of the spectral functions which would allow an experimental discrimination between correlation-driven partial localization and a usual filled-band scenario. We lay emphasis on the role of orbital degeneracies and on intra-atomic correlations which compete with the (anisotropic) kinetic energy. The features chosen for discussion are the distribution of spectral weight, the formation of coherent bands, and the opening of an excitation gap.

We begin the discussion in Sec. II with a brief exposition of the model Hamiltonian and the techniques emphasizing the general structures involved. The numerical procedure and the parameters adopted in the actual calculation are the presented in Sec. III. In the subsequent sections IV and V, we delineate details of the models and the results obtained. The conclusions are summarized in Sec. VI.

II. MODEL HAMILTONIAN AND COMPUTATIONAL METHOD

For the adoption of a model describing the $5f$ electrons in actinide-based heavy-fermion systems we rely on experience with *ab initio* electronic-structure calculations. In these materials, the direct overlap of the $5f$-wave functions at neighboring sites is anticipated to be rather small due to the large U-U distance. Detailed studies[18] suggest that the $5f$ states acquire their dispersion by hybridization with high-lying empty conduction states. We model these processes by introducing weak effective transfer integrals. The interplay between intra-atomic Coulomb interaction and anisotropic kinetic energy in $5f$ systems is described by the simple model Hamiltonian[12]

$$H = H_{\text{band}} + H_{\text{Coul}}. \tag{1}$$

The local Coulomb repulsion

$$H_{\text{Coul}} = \frac{1}{2}\sum_a \sum_{j_{z_1},\ldots,j_{z_4}} U_{j_{z_1}j_{z_2}j_{z_3}j_{z_4}} c^\dagger_{j_{z_1}}(a) c^\dagger_{j_{z_2}}(a) c_{j_{z_3}}(a) c_{j_{z_4}}(a) \tag{2}$$

is written in terms of the usual fermionic operators $c^\dagger_{j_z}(a)$ $[c_{j_z}(a)]$ which create [annihilate] an electron at site a in the $5f$ state with total angular momentum j and z projection j_z. Considering the fact that the spin-orbit splitting is large we neglect contributions from the excited spin-orbit multiplet $j=7/2$ and adopt the j-j coupling scheme. The Coulomb matrix elements $U_{j_{z_1}j_{z_2}j_{z_3}j_{z_4}}$ for $j_{zi}=-5/2,\ldots,5/2$,

$$U_{j_{z_1}j_{z_2}j_{z_3}j_{z_4}} = \delta_{j_{z_1}+j_{z_2},j_{z_3}+j_{z_4}} \sum_J U_J C^{JJ_z}_{5/2,j_{z1};5/2,j_{z2}} C^{JJ_z}_{5/2,j_{z3};5/2,j_{z4}}, \tag{3}$$

are given in terms of the usual Clebsch-Gordan coefficients $C^{\cdots}_{\cdots}$ and the Coulomb parameters U_J.

The kinetic energy operator in the band term H_{band} describes the hopping between all pairs neighboring sites $\langle ab\rangle$:

$$H_{\text{band}} = -\sum_{\langle ab\rangle, j_z} t_{j_z}[c^\dagger_{j_z}(a)c_{j_z}(b) + \text{H.c.}] + \sum_{a,j_z} \epsilon_f c^\dagger_{j_z}(a) c_{j_z}(a). \tag{4}$$

We assume the transfer integrals t_{j_z} to be diagonal in the orbital index j_z. This simplification is justified for a one-dimensional system since the cylindrical symmetry allows one to select a common quantization axis for all sites. We would like to stress that although the hopping term is assumed to be diagonal in the orbital indices, the corresponding channels are coupled through the Coulomb term. Finally, we account for the orbital energy ϵ_f which determines the f valence of the ground state.

The single-particle spectral function

$$A_{j_z}(k,\omega) = \begin{cases} \sum_n |\langle \Psi^{(N+1)}_n | c^\dagger_{j_z}(k) | \Psi^{(N)}_0 \rangle|^2 \delta(\omega - \omega^{(+)}_{n0}), & \omega > 0, \\ \sum_n |\langle \Psi^{(N-1)}_n | c_{j_z}(k) | \Psi^{(N)}_0 \rangle|^2 \delta(\omega + \omega^{(-)}_{n0}), & \omega < 0, \end{cases} \tag{5}$$

with

$$c_{j_z}(k) = \frac{1}{\sqrt{L}} \sum_a e^{ika} c_{j_z}(a), \quad \omega^{(\pm)}_{n0} = E^{(N\pm1)}_n - E^{(N)}_0, \tag{6}$$

yields the probability for adding ($\omega>0$) or removing ($\omega<0$) an electron with energy ω in a state characterized by momentum k and angular momentum projection j_z to the N-particle ground state $|\Psi^{(N)}_0\rangle$ with energy $E^{(N)}_0$. The states with $N\pm1$ and their energies are denoted by $|\Psi^{(N\pm1)}_n\rangle$ and $E^{(N\pm1)}_n$, respectively, and L is the number of sites.

The importance of the spectral functions stems, first, from the fact that they can be observed in photoemission and inverse photoemission experiments and, second, that the orbital-projected expectation value of the kinetic energy per site,

$$T_{j_z} = \int_{-\infty}^{+\infty} d\omega f(\omega) \frac{1}{L} \sum_k \epsilon_{j_z}(k) A_{j_z}(k,\omega), \tag{7}$$

as well as the orbital-projected momentum distribution function

$$n_{j_z}(k) = \int_{-\infty}^{+\infty} d\omega f(\omega) A_{j_z}(k,\omega) \tag{8}$$

and the orbital-projected density of states (DOS)

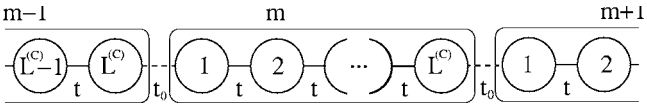

FIG. 1. Representation of a one-dimensional chain as a superlattice of identical $L^{(C)}$-site clusters. The orbital-dependent transfer integrals between neighboring sites within a cluster and between adjacent clusters are $t=(t_{j_z=-5/2},\ldots,t_{j_z=5/2})$ and $t_0=(t_{0j_z=-5/2},\ldots,t_{0j_z=5/2})$, respectively.

$$D_{j_z}(\omega)=\frac{1}{L}\sum_k A_{j_z}(k,\omega), \tag{9}$$

can be expressed through them. The dispersion of the band energies $\epsilon_{j_z}(k)$ is given by the kinetic energy, Eq. (4), and f is the usual Fermi function.

We determine the spectral function $A_{j_z}(k,\omega)$ from the single-particle Green's function $G_{j_z}(k,\omega)$,

$$A_{j_z}(k,\omega)=-\frac{1}{\pi}\lim_{\eta\to 0^+}\mathrm{Im}\,G_{j_z}(k,\omega+i\eta), \tag{10}$$

which, in turn, are calculated applying cluster perturbation theory (CPT).[19–23] The method which has been successfully applied to a wide variety of many-particle models proceeds by dividing the infinite periodic lattice into identical finite $L^{(C)}$-site clusters as illustrated in Fig. 1.

The Hamiltonian (1) takes the form

$$H=\sum_m H_m^0+\sum_{m,n,a,b,j_z} V_{abj_z}^{mn} c_{maj_z}^{\dagger} c_{nbj_z}, \tag{11}$$

where H_m^0 refers to cluster m while $V_{abj_z}^{mn}$ describes the hopping between sites a and b on the adjacent clusters m and n. The Green's functions of the finite clusters,

$$(\hat{G}_{j_z}^{(C)}(z))_{ab}=G_{abj_z}^{(C)}(z),\quad a,b=1,\ldots,L^{(C)}, \tag{12}$$

are calculated exactly, thereby fully accounting for the complex dynamics of the strongly correlated system. Here we use the locator representation where the indices refer to the sites in the cluster. In a second step, the intercluster hopping $V_{abj_z}^{mn}$ is treated as a weak perturbation which yields the Green's function of the superlattice:[19,20]

$$G_{abj_z}(Q,z)=\left(\frac{\hat{G}_{j_z}^{(C)}(z)}{1-\hat{V}_{j_z}(Q)\hat{G}_{j_z}^{(C)}(z)}\right)_{ab}. \tag{13}$$

The variation with the wave vector Q which is taken from the first Brillouin zone of the superlattice is introduced by the intercluster hopping matrix $\hat{V}_{j_z}(Q)$. Its matrix elements are obtained from $V_{abj_z}^{mn}$ by performing a Fourier transformation with respect to the cluster indices m and n. Following Ref. 19, the translational invariance of the original lattice is explicitly restored, yielding the Green's function

$$G_{j_z}(k,z)=\frac{1}{L^{(C)}}\sum_{a,b} e^{-ik(a-b)}G_{abj_z}(L^{(C)}k,z). \tag{14}$$

Note that the CPT is exact in three limiting cases: vanishing hopping terms, in an uncorrelated system, and for infinite cluster size. The approximation is controlled most effectively by considering different cluster sizes $L^{(C)}$

Before we turn to a detailed description of the calculations we would like to mention the following caveat. The formulation of CPT as summarized above implicitly relies on the assumption that the ground states of the interacting electron system are nondegenerate. This proposition, however, may not be satisfied for the building blocks of the superlattice. The problem arises trivially for clusters containing an odd number of electrons where all states are at least twofold degenerate. Of course one could try to circumvent the problem by choosing appropriate cluster sizes or by varying the band filling—i.e., the number of particles. This strategy which may work for simple systems does not provide a solution in orbitally degenerate systems. Due to the local orbital degrees of freedom, the complexity increases rapidly with the number of sites or particles imposing serious restrictions on models. As we attempt at a description of homogeneous phases we separately calculate the Green's functions for the states of the ground-state manifold and subsequently average the spectral function.

III. COMPUTATIONAL DETAILS

We begin by specifying the model parameters entering the Hamiltonian, Eq. (1). The high-energy scale is set by the Coulomb repulsion between two $5f$ electrons at the same site. The parameters U_J are chosen according to the following considerations. First, it is well known that the isotropically averaged Coulomb repulsion in a metal is strongly reduced as compared to its value in an atom. The reduction is a direct consequence of screening by the itinerant conduction electrons which, in turn, implies that the actual value depends upon the chemical environment of the correlated ion under consideration. We do not attempt an *ab initio* calculation of this quantity but rather leave it as a parameter U_{at} whose value can be estimated from the positions of the valence peaks in photoemission and inverse photoemission. The intra-atomic correlation which is the focus of interest in the present paper involves the anisotropic parts of the Coulomb interaction. The latter give rise to the multiplet structure. It is important to note that the corresponding interactions are (usually) not screened and hence retain their atomic values. As we expect the anisotropic Coulomb parameters to be rather robust with respect to changes in the chemical composition or to pressure we use fixed values for the differences

$$\Delta U_4=U_{J=4}-U_{J=0}=-3.79\ \mathrm{eV},$$

$$\Delta U_2=U_{J=2}-U_{J=0}=-2.72\ \mathrm{eV}, \tag{15}$$

which were determined from an *ab initio* calculation for UPt_3.[24] The value for the orbital energy ϵ_f in Eq. (4) is fixed by the requirement that low-energy states be formed by lin-

ear combinations of the ionic f^2 and f^3 configurations which are energetically (almost) degenerate. The intermediate valent ground state with $n_f \simeq 2.5$ allows for low-energy valence transitions and the formation of bands also in the strong-coupling limit.

Finally, the values of the transfer integrals t_{j_z} are varied in the strong-coupling regime. As in Ref. 12 we choose $t_{1/2} = t_{5/2}$ in the figures.

We next turn to the calculation of the cluster Green's functions $\hat{G}^{(C)}_{j_z}(z)$ which account for the local correlated dynamics. We should like to mention that the use of the open-boundary conditions required by the CPT method considerably increases the numerical effort over that encountered in finite clusters with periodic boundary conditions. A further difficulty arises from the fact that the orbital degrees of freedom may lead to a rather high density of low-energy states. Keeping in mind these complications the Green's functions for clusters with two and three correlated sites are calculated using Lanczos continued-fraction technique.[25] To avoid convergence problems due to the near degeneracy of the lowest excited states in the $5f$ systems we use the JDQR algorithm[26] instead of the usual Lanczos method to obtain the ground state.

For purposes of comparison we present alongside the CPT spectra the test cases of finite clusters using periodic-boundary conditions. In this case, the calculation of the cluster Green's function $\hat{G}^{(C)}_{j_z}(z)$ simplifies to

$$G^{(C)}_{abj_z}(z) = \frac{1}{L}\sum_{k_\ell=1}^{k_L} e^{ik_\ell(a-b)} G^{(C)}_{j_z}(k_\ell, z), \tag{16}$$

where[27]

$$G^{(C)}_{j_z}(k,z) = G^{(C)}_{j_z,e}(k,z) + G^{(C)}_{j_z,h}(k,z),$$

$$G^{(C)}_{j_z,e}(k,z) = \langle \Psi_0 | c_{j_z}(k) \frac{1}{z - H + E_0} c^\dagger_{j_z}(k) | \Psi_0 \rangle,$$

$$G^{(C)}_{j_z,h}(k,z) = \langle \Psi_0 | c^\dagger_{j_z}(k) \frac{1}{z + H - E_0} c_{j_z}(k) | \Psi_0 \rangle. \tag{17}$$

The discrete value $k_\ell = \ell(2\pi/L)$, $\ell = 0, \ldots, L-1$, labels the single-particle eigenstates of the L-site cluster. The Green's functions are evaluated for complex frequencies $z = \omega + i\eta$ with $\eta > 0$. The imaginary part leads to additional Lorentzian broadening of the spectral functions and may affect the behavior of the integrals like the expectation value of the kinetic energy or the momentum distribution function. All these quantities are increasingly difficult to compute as η decreases. For the actual calculations we choose values for η of the order of 10^{-2} of the relevant hopping integrals. For the plots a rather large value of $\eta = 0.03$ is chosen to allow for a good visualization.

The absolute values of U_f are very large compared to the hopping integral, and thus we shall limit ourselves to the subspace of f^2 and f^3 configurations for the ground state which has shown to be a good approximation. This leads to a considerable reduction of Hilbert-space dimension and less computational costs. The actual sizes of the Hilbert spaces in the reduced systems for the two-site cluster filled with five electrons are 600 states and 220 and 400, respectively, for four and five electrons. For the clusters with three sites one obtains 18 000 dimensions for a filling with eight electrons and 8000 and 13 500, respectively, for seven and nine electrons. The matrix representations of the Hamiltonian are then stored as sparse matrices.

IV. SPECTRAL FUNCTIONS OF FINITE CLUSTERS

A. Atomic limit

We begin by discussing the spectral function of our model in the atomic limit neglecting hopping between the sites. The results provide a first qualitative insight into the behavior in the strong-coupling limit. Due to the rotational invariance of the Coulomb interaction, Eq. (2), the spectral functions $A_{j_z}(\omega)$ will not depend on the magnetic quantum number j_z. The lowest-energy states of an intermediate-valent system in the zero-bandwidth limit are given by products of atomic f^2 and f^3 configurations whose energies are assumed to be (almost) degenerate. The corresponding spectral functions are obtained in close analogy to the classical work by Hubbard.[28] The zero-configuration width approximation which neglects intra-atomic correlations leads to a characteristic three-peak structure. The valence transitions $f^2 \to f^1$ and $f^3 \to f^4$ occur at large energies and, concomitantly, do not affect the low-temperature behavior. The latter is determined by the low-energy peak resulting from the transitions $f^2 \leftrightarrow f^3$ within the f^2 and f^3 configurations. This peak is a direct consequence of the intermediate-valent ground state. The strong correlations present imply a substantial transfer of spectral weight from the low-energy part to the high-energy regime. The weights of the peaks can be estimated from combinatorial considerations. The weight $Z(f^2 \to f^1)$ of the transition $f^2 \to f^1$ equals the probability that a state with a given j_z is occupied in that f^2 contribution of the mixed-valent ground state. Following these lines one finds

$$Z(f^2 \to f^1) = \frac{1}{6}, \quad Z(f^2 \to f^3) = \frac{1}{3},$$

$$Z(f^3 \to f^2) = \frac{1}{4}, \quad Z(f^3 \to f^4) = \frac{1}{4}. \tag{18}$$

The central focus of the present paper is the evolution of the low-energy peak whose spectral weight sums up to 7/12. Intra-atomic correlations which are usually described by Hund's rules further reduce the spectral weight of the low-energy excitations involving valence transitions $|f^3, J = 9/2\rangle \rightleftharpoons |f^2, J = 4\rangle$ between the ground-state multiplets. The corresponding spectral weights can be expressed in a straightforward way in terms of the usual Clebsch-Gordan coefficients and the reduced matrix elements. In addition to the central peak one finds transitions to the excited multiplets $|f^3, J = 9/2\rangle \to |f^2, J = 2\rangle$ and $|f^2, J = 4\rangle \to |f^3, J = 3/2\rangle$, $|f^3, J = 5/2\rangle$ occurring at the corresponding multiplet excitations. The excitation energies as well as the corresponding spectral weights are listed in Table I. We should like to mention that

TABLE I. Positions and spectral weight of the atomic transitions in uranium from numerical calculations. For $\omega \leqslant 0$ eV eV the contributions are from the hole propagation and for $\omega \geqslant 0$ eV eV from the particle propagation.

	PES			BIS	
Position/eV	−1.06	0.00	0.00	1.60	2.73
Spectral weight	0.054	0.196	0.218	0.032	0.083

there is no transition into the excited multiplet $|f^2, J=0\rangle$.

B. Results for finite clusters

We next turn to the modifications introduced by the hopping between different sites which acts as a weak perturbation in the strong-coupling limit. Its principal effect is to remove the rotational symmetry of the isolated atom and, consequently, remove the high degeneracy of the ground state. As the total angular momentum ceases to be a good quantum number the ground state may contain admixtures from excited J multiplets. The model Hamiltonian as specified by Eqs. (1)–(4), however, conserves the z component of the angular momentum, allowing us to classify the eigenstates with respect to J_z. The magnetic character of the ground states depends upon the transfer integrals as shown in Ref. 12. These modifications affect the spectral functions $A_{j_z}(k_\ell, \omega)$ of an L-site cluster where the discrete set of quantum numbers $k_\ell = 0, \ldots, (L-1)2\pi/L$ labels the single-particle eigenstates. First, the positions of the peaks corresponding to the transitions between different valence states may acquire dispersion. Second, spectral weight may be transferred from the low-energy regime to high-energy satellites. Third, transitions to excited multiplets not present in the atomic limit may appear and, finally, the overall spectral weight may be redistributed among the different j_z channels. These issues will be addressed in the following section.

A first qualitative understanding can be gained by considering the spectral functions of a two-site cluster where simple approximate expressions are found for the ground states in limiting cases. Throughout the discussion we restrict ourselves to the strong-coupling regime $|t_{j_z}| \ll |\Delta U_J|$ where the ground state is mainly built from products of local f^2 configurations $|f^2; 4J_z\rangle$ and local f^3 configurations $|f^3; 9/2 J'_z\rangle$. Finite hopping between the two sites a and b splits the manifold in first-order perturbation theory. We consider the case of strongly anisotropic hopping $|t_{3/2}| = |t| \gg |t'| = |t_{5/2}| = |t_{1/2}|$ and $|t_{3/2}| = |t| \ll |t'| = |t_{5/2}| = |t_{1/2}|$ as well as isotropic hopping $t_{3/2} = t = t' = t_{5/2} = t_{1/2}$. The variation with t, t' of the spectral functions is displayed in Fig. 2.

Let us first consider the behavior along the isotropic line $t_{3/2} = t = t' = t_{5/2} = t_{1/2}$. Due to the rotational invariance, the magnitude $\mathcal{J}^2$ of the total angular momentum $\mathcal{J} = J(a) + J(a)$ provides a good quantum number. It has been shown previously[12] that the ground state is sixfold degenerate. It is a linear combinations of the $\mathcal{J}^2$ eigenstates $|(\frac{9}{2}4)\mathcal{J}\mathcal{J}_z\rangle$ and $|(4\,9)\mathcal{J}\mathcal{J}_{2z}\rangle$ for $\mathcal{J} = 5/2$ which can be expressed in terms of the above-mentioned product states $|f^3; \frac{9}{2}\mathcal{J}_z - J_z\rangle |f^2; 4J_z\rangle$ and

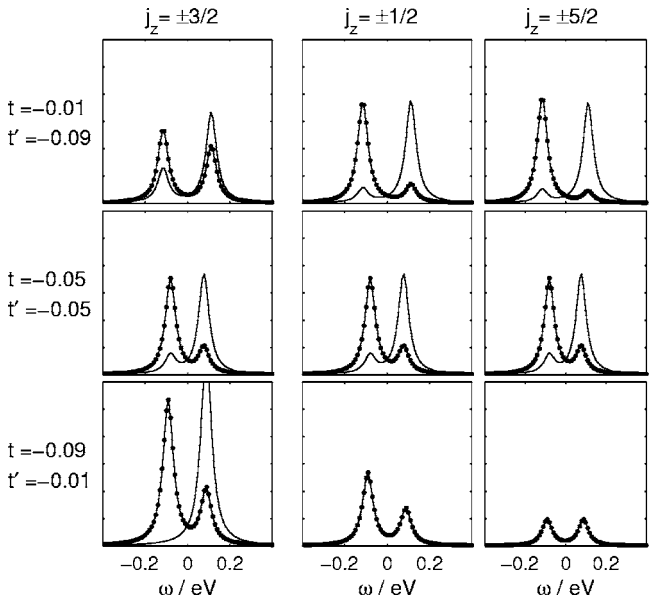

FIG. 2. Variation with wave number of the orbital-projected spectral functions calculated for a two-site cluster with five electrons and the hopping parameters $t_{3/2} = t$ and $t_{1/2} = t_{5/2} = t'$. The solid line and the dotted line refer to $k = 0$ and $k = \pi$, respectively. The spectra are obtained from averaging the Green's functions over the degenerate ground-state manifold. Spectral weight is transferred to local excitations (valence transitions and transitions into excited atomic multiplets) which are not displayed here. The Lorentzian broadening is $\eta = 0.03$.

$|f^2; 4J_z\rangle |f^3; \frac{9}{2}\mathcal{J}_z - J_z\rangle$. The gain in kinetic energy,

$$|t| \left| \left\langle \left(\frac{9}{2}4\right)\mathcal{J}\mathcal{J}_z \middle| \sum_{j_z} c^\dagger_{j_z}(a) c_{j_z}(b) \middle| \left(4\frac{9}{2}\right)\mathcal{J}\mathcal{J}_z \right\rangle \right| = |t| \frac{33}{14} |\tau(\mathcal{J})|, \tag{19}$$

given in terms of the reduced matrix element $\left(\frac{9}{2}\middle\| c^\dagger_{j_z} \middle\| 4\right) = \sqrt{\frac{33}{14}}$ and the $6j$ symbol

$$\tau(\mathcal{J}) = (-1)^{\mathcal{J}} 10 \begin{pmatrix} 4 & \frac{5}{2} & \frac{9}{2} \\ 4 & \mathcal{J} & \frac{9}{2} \end{pmatrix} \tag{20}$$

for $\mathcal{J} = 5/2$, results from the formation of symmetric (antisymmetric) combinations the above-mentioned $\mathcal{J}^2$ eigenstates. The isotropy of the ground state is reflected in the isotropic spectral functions which exhibit peaks at the energies

$$\pm \frac{33}{14} \frac{907}{1386} t = \pm 0.077 \text{ eV}. \tag{21}$$

Due to the strong correlations, we find two peaks for both removing (adding) electrons in symmetric states $c^\dagger_{j_z}(k=0)$ and antisymmetric states $c^\dagger_{j_z}(k=\pi)$.

In the strongly anisotropic case $|t_{3/2}| = |t| \gg |t'| = |t_{5/2}| = |t_{1/2}|$, the wave function of the Kramers' degenerate ground state with $\mathcal{J}_z = \pm 15/2$ has the simple form (for $\mathcal{J}_z = +15/2$)

$$|\Psi\rangle_{15/2} = \frac{1}{\sqrt{2}}\left(c^{\dagger}_{3/2}(a) + \frac{t}{|t|}c^{\dagger}_{3/2}(b)\right)$$
$$= c^{\dagger}_{5/2}(a)c^{\dagger}_{1/2}(a)c^{\dagger}_{5/2}(b)c^{\dagger}_{1/2}(b) \quad (22)$$

describing an independent $j_z=3/2$ electron in a magnetically polarized background. This state is separately an eigenstate of the kinetic energy as well as the Coulomb energy. Removing an electron in the single-particle state

$$\frac{1}{\sqrt{2}}\left(c^{\dagger}_{3/2}(a) + \frac{t}{|t|}c^{\dagger}_{3/2}(b)\right)$$

as well as adding one in its orthogonal counterpart leads to final states $J(a)=4=J(b)$ and $J(a)=9/2=J(b)$, respectively, where both sites are in the ground-state multiplets of the local f^2 and f^3 configurations. As a consequence, we find two sharp peaks with full spectral weight at the energies $\omega=\pm|t|$ which evolve into a quasiparticle band in extended systems. The additional spectral weight appearing in Fig. 2 at positive energies $\omega=+|t|$ accounts for the probability of adding an electron in the minority channel $j_z=-3/2$. This generates final states which contain contributions from excited states like unfavorable local f^4 configurations and excited multiplets in the local f^3 subspaces. The overlap with states from the local ground-state manifold gives rise to a peak at $\omega=+|t|$ whose reduced height, however, highlights the transfer of significant spectral weight to the high-energy regime. Finally, the absence of dispersion in the $j_z=1/2$ and $j_z=5/2$ spectral functions as well as the reduced spectral weight in the low-energy regime reveals the localized character of the corresponding orbitals in the ground state. The evolution of the spectra and in particular the reduction of spectral weight in the low-energy regime are reminiscent of the gap formation at the Mott-Hubbard transition. The qualitative difference between the 5/2 and 1/2 channels as well as the asymmetry within the 1/2 channel reflects the intra-atomic (Hund's rule type) correlations.

The structure of the spectral functions in the complementary anisotropic limit $|t_{5/2}|=|t_{1/2}|=|t'|\gg|t|=|t_{3/2}|$ can be explained by similar considerations. The Kramers' degenerate ground state is built from configurations where all but the $j_z=-3/2(j_z=3/2)$ orbitals are occupied. This implies $\mathcal{J}_z=\pm 3/2$. It is important to note that this implies antiferromagnetic correlations between the sites. In this state, delocalization of the $j_z=3/2(j_z=-3/2)$ is not principally excluded. It is, however, associated with breaking Hund's rules. As a result we find dispersion in the corresponding channels. The spectral weight, however, is reduced due to intra-atomic excitations.

The characteristic structure of the spectra as summarized above is present also in the three-site cluster as can be seen from Fig. 3. The coherence effects, however, are more pronounced. For a discussion of the (approximate) ground states in limiting cases we refer the reader to Ref. 12.

A striking feature is the splitting of the lower peaks for $j_z=\pm 1/2$ and $j_z=\pm 5/2$ at $t_{1/2}=t_{5/2}=-0.09$ and $t_{3/2}=-0.01$. The key to the explanation is provided by the observation that the corresponding ground state is characterized by antiferromagnetic intersite correlations, a property encountered already in the two-site cluster discussed above. The implications for the three-site system, however, are more subtle. For periodic boundary conditions the ground state is a complex superposition of several (almost) equivalent states reflecting frustration. Removing an electron from the ground state leads to rather complex final states which, in turn, give rise to the observed splitting.

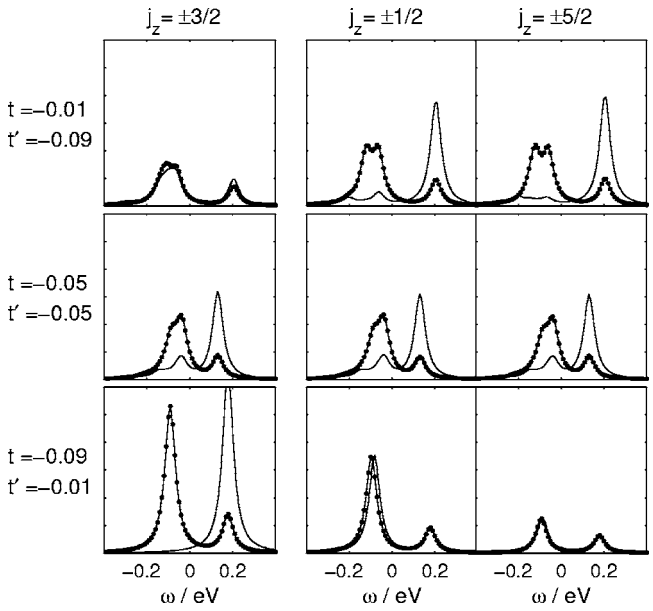

FIG. 3. Variation with wave number of the orbital-projected spectral functions calculated for a three-site cluster with eight electrons and the hopping parameters $t_{3/2}=t$ and $t_{1/2}=t_{5/2}=t'$. The solid line and dotted line refer to $k=0$ and $k=\pm 2\pi/3$, respectively. The spectra are obtained from averaging the Green's functions over the degenerate ground-state manifold. Spectral weight is transferred to local excitations (valence transitions and transitions into excited atomic multiplets) which are not displayed here. The Lorentzian broadening is $\eta=0.03$.

The most prominent feature of the spectral functions in the strongly anisotropic limit is the partial localization which can be viewed as an orbital-selective Mott transition. The intra-atomic correlations strongly enhance the anisotropies of the kinetic energy as can be seen from Fig. 4. The calculated projected kinetic energy T_{j_j}/t_{j_z} (Fig. 4) agrees well with results from ground-state wave function.[12] The small differences in the results from the ground-state wave function are due to Lorentzian broadening with $\eta=0.005$.

V. CLUSTER PERTURBATION THEORY

The essential benefit gained from CPT is the possibility to calculate the spectral functions at arbitrary wave vectors and band filling. In the present paper we explore the first aspect, treating CPT as a sophisticated interpolation scheme for the variation with k. The averaged particle number per site, on the other hand, is kept fixed at the value used in the underlying cluster calculation. Comparing the spectra of the infinite chain to those of isoelectronic finite clusters provides us with an estimate of finite-size effects since the building blocks of the chain are treated with different boundary conditions.

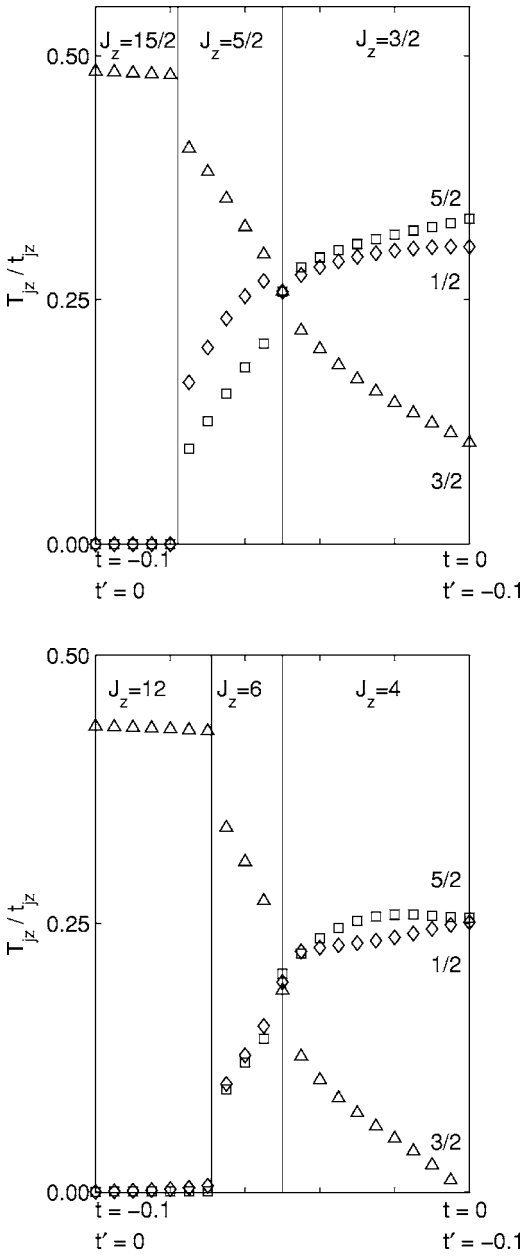

FIG. 4. Ratio $T_{j_z}/t_{j_{j_z}}$ of the two-site cluster (left) and three-site cluster (right) with $t_{j_z}<0$ along the line $t_{3/2}=t$ and $t_{1/2}=t_{5/2}=t'$ connecting the values below the figures.

The qualitative behavior of the spectral functions reflects the detailed structure of ground state which is determined by the competition between the energy gain due to intra-atomic correlations and kinetic energy. The latter, however, depends upon the boundary conditions imposed upon the wave functions. The cluster calculations discussed in the preceding section were performed adopting the usual periodic-boundary conditions. The CPT, however, requires cluster Green's function for open-boundary conditions. In the strong-coupling regime, the dependence upon the transfer integrals of the ground state is only weakly affected by the actual choice of boundary conditions. In the strongly anisotropic limit with one dominating transfer integral (a) the high-spin states with ferromagnetic intersite correlations are energetically most favorable. They are followed by rather complex intermediate-spin states (b) as the case of isotropic hopping (c) is approached. Along this line the salient feature of the correlated ground state is its high degeneracy. In the case of two dominating hopping channels (d) low-spin phases with antiferromagnetic intersite correlations are formed. These features originally derived for periodic-boundary conditions are encountered also for open-boundary conditions as can be deduced from Fig. 5.

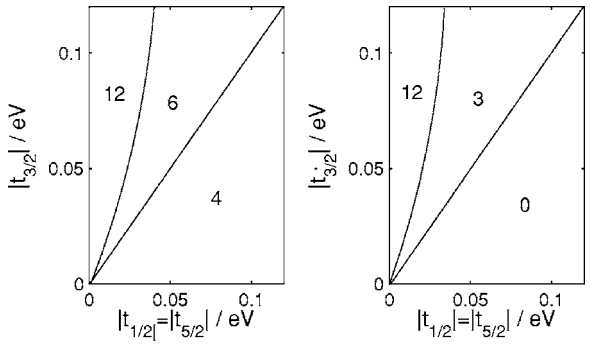

FIG. 5. Phase diagrams of the three-site cluster filled with eight electrons for negative hopping parameters t_{j_z}, derived for the total magnetization J_z for periodic-boundary conditions (left panel) and open-boundary conditions (right panel).

Figures 6 and 7 display the orbital-projected spectral functions of the linear chain. The data refer to the low-energy regime where the electronic excitations involve transitions between the lowest Hund's rule multiplets. We adopt the same values for the transfer integrals as in the cluster calculations. The system is clearly in the strong-coupling regime

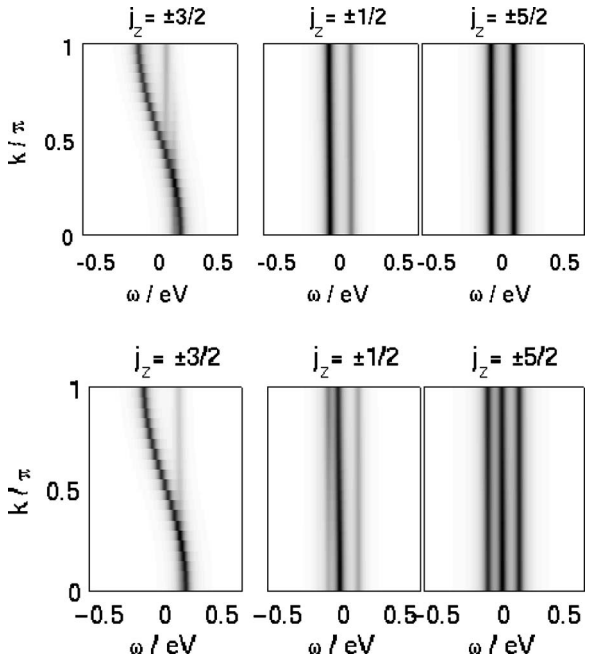

FIG. 6. Spectral functions of a one-dimensional 5*f* system from the *CPT* with cluster of two sites (upper panel) and three sites (lower panel). The orbital-projected spectra are a superposition of the $+j_z$ and $-j_z$ parts of the spectra. The anisotropic hopping parameters are $t_{3/2}=-0.09$ eV and $t_{1/2}=t_{5/2}=-0.01$ eV. The peaks are broadened with a finite imaginary part of $\eta=0.03$.

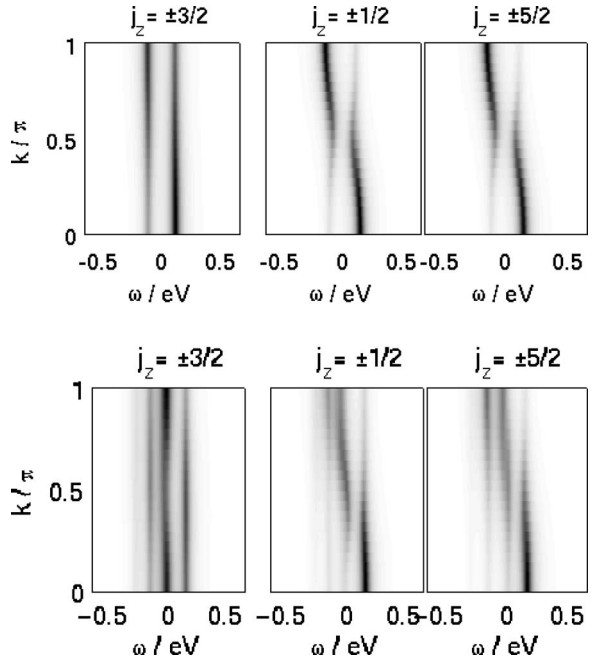

FIG. 7. Spectral functions of a one-dimensional $5f$ system from the *CPT* with cluster of two sites (upper panel) and three sites (lower panel). The orbital-projected spectra are a superposition of the $+j_z$ and $-j_z$ parts of the spectra. The anisotropic hopping parameters are $t_{3/2}=-0.01$ eV and $t_{1/2}=t_{5/2}=-0.09$ eV. The peaks are broadened with a finite imaginary part of $\eta=0.03$.

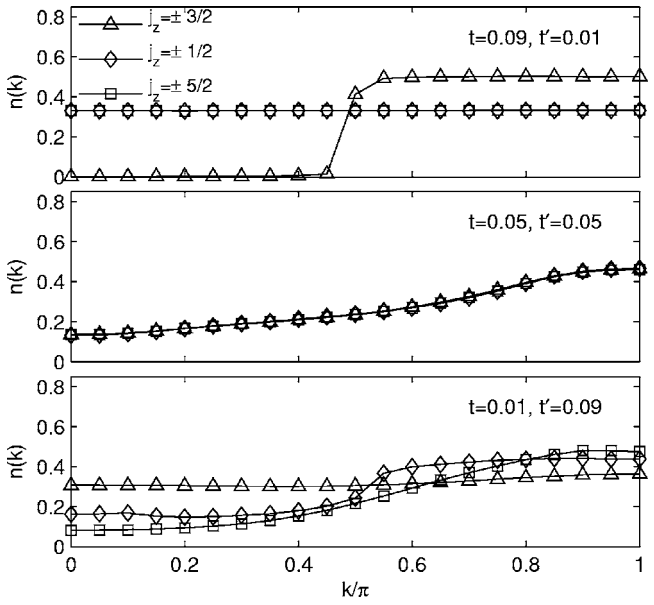

FIG. 8. Orbital-projected MDF calculated within CPT starting from three-site cluster and the hopping parameters $t_{3/2}=t$ and $t_{1/2}=t_{5/2}=t'$. The spectral functions displayed in the figure were integrated over energy in an interval of −4 eV below the chemical potential.

where the symmetries of the ground states are rather sensitive to the detailed description of the kinetic energy. The high-energy features associated with transitions to excited atomic states are not shown here.

As regards the variation with wave vector of the spectral functions, the qualitative behavior closely parallels the one obtained for the finite clusters. The spectral functions clearly show a dispersing band in the orbital channel with the dominant hopping. The position of the narrow peak whose finite width is to be attributed to the additional broadening follows the characteristic cosine dispersion of a one-dimensional tight-binding band with nearest-neighbor hopping. The gap in the dispersion of the dominant hopping channel in Figs. 6 and 7 are introduced by the antiferromagnetic intersite correlations which effectively reduce the size of the Brillouin zone. The bandwidth, however, is reduced by a factor of $\sim 7/12$ as compared to $4|t|=0.36$ eV expected for uncorrelated electrons. The renormalization reflects the transfer of spectral weight to the high-energy satellites. The linewidths of the dispersing bands in the linear chain are approximately twice the value of the bonding-antibonding splitting in the two-site cluster. This discrepancy is due to the fact that the number of nearest neighbors in the lattice is twice that in the corresponding cluster. The $5f$ channels with subdominant hopping exhibit low-energy excitations which are incoherent and which may exhibit a pseudogap at the Fermi energy. It should be noted that the CPT spectra based on three-site clusters are in good agreement with their two-site cluster counterparts. The cluster size and the boundary conditions apparently affect the incoherent excitations in the channels with the subdominant hopping. This can be seen from comparing the CPT spectra obtained from two- and three-site clusters.

The coexistence of a coherent $5f$ band and incoherent f-derived low-energy excitations implies partial localization. The orbital-selective localization suggests the presence of different types of low-energy excitations which have different orbital character. Photoemission experiments with polarized incident light should be able to distinguish the two. In fact, recent experiments on URu_2Si_2 seem to be consistent with this hypothesis.

The momentum distribution function (MDF) as defined in Eq. (8) is displayed in Fig. 8. The variation with wave vector k clearly shows the dual character of the $5f$ electrons. In the homogeneous high-spin phase, the height of the discontinuity in $n_{j_z}(k)$ for orbitals with dominant hopping is consistent with the spectral weight of the dispersive low-energy peak. In the low-spin phase, however, it reflects the reduction of the Brillouin zone due to antiferromagnetic correlations.

Figure 9 displays the orbital-projected DOS as calculated within CPT.

VI. SUMMARY AND OUTLOOK

We have studied the consequences of strong intra-atomic correlations on the spectral functions of $5f$ electrons by applying CPT. The result derived for a one-dimensional chain confirms the idea of orbital-dependent localization in anisotropic systems. The orbital-projected spectral functions for the channels with dominant hopping display narrow dispersive bands in the vicinity of the Fermi energy while the low-energy single-particle excitations in the remaining channels involve mainly incoherent local transitions. In all channels, considerable spectral weight is transferred to the high-energy

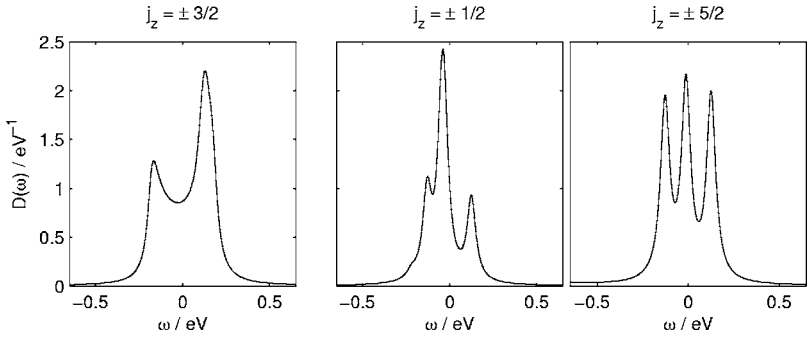

FIG. 9. Orbital projected density of states $D_{j_z}(\omega)$ of a one-dimensional $5f$ system from the *CPT* with cluster of three sites. The anisotropic hopping parameters are $t_{3/2}=-0.09$ eV and $t_{1/2}=t_{5/2}=-0.01$ eV. The peaks are broadened with a finite imaginary part of $\eta=0.03$.

regime where we find intra-atomic transitions to excited multiplets as well as valence transitions. The transfer of spectral weight renormalizes the widths of the dispersing bands and hence increases the corresponding effective masses.

The dual character of the $5f$ electrons—i.e., the division of $5f$ states into delocalized and localized orbitals—can be clearly seen from the orbital-projected momentum distribution function. The latter has a pronounced discontinuity for the orbitals with dominant hopping while its smooth variation can almost be neglected in the remaining channels. In a three-dimensional crystal such a behavior implies that only the orbitals with dominant hopping contribute to the quantum oscillations of the dHvA effect.

Calculations starting from clusters with two and three sites yield similar results in the strong-coupling regime. The orbital-dependent suppression of the kinetic energy calculated for the chain agrees well with previous results obtained for small finite clusters imposing periodic-boundary conditions. These finding suggest that the features associated with orbital-selective localization are rather robust.

The model calculations presented suggest that the orbital dependence of the $5f$ spectral functions can be used as fingerprint for orbital-selective localization in actinide systems. The orbital dependence could be observable by varying the polarization of the incident light.

It is therefore desirable to perform similar calculations for models describing real materials. This requires the calculations to be extended to higher dimensions. An important generalization is the inclusion of nondiagonal transfer integrals which is currently in progress.

[1] P. Thalmeier and G. Zwicknagl, *Handbook on the Physics and Chemistry of Rare Earths* (Elsevier B. V., Amsterdam, 2005), Vol. 34, p. 135.
[2] J. W. Allen, *Resonant Photoemission of Solids with Strongly Correlated Electrons*, Vol. 1 of Synchrotron Radiation Research: Advances in Surface and Interface Science (Plenum Press, New York, 1992), Chap. 6, p. 253.
[3] S. ichi Fujimori *et al.*, J. Electron Spectrosc. Relat. Phenom. **101-103**, 439 (1999).
[4] A. J. Arko *et al.*, J. Less-Common Met. **133**, 87 (1987).
[5] R. Eloirdi, T. Gouder, F. Wastin, J. Rebizant, and F. Huber (unpublished).
[6] H. Kumigashira, T. Ito, A. Ashihara, H.-D. Kim, H. Aoki, T. Suzuki, H. Yamagami, T. Takahashi, and A. Ochiai, Phys. Rev. B **61**, 15707 (2000).
[7] G. Zwicknagl and P. Fulde, J. Phys.: Condens. Matter **15**, S1911 (2003).
[8] G. Zwicknagl, A. Yaresko, and P. Fulde, Phys. Rev. B **68**, 052508 (2003).
[9] A. Hiess *et al.*, cond-mat / 0411041 (unpublished).
[10] L. Petit, A. Svane, W. M. Temmerman, Z. Szotek, and R. Tyer, Europhys. Lett. **62**, 391 (2003).
[11] J. M. Wills, O. Eriksson, A. Delin, P. H. Andersson, J. J. Joyce, T. Durakiewicz, M. T. Butterfield, A. J. Arko, D. P. Moore, and L. A. Morales, J. Electron Spectrosc. Relat. Phenom. **135**, 163 (2004).
[12] D. V. Efremov, N. Hasselmann, E. Runge, P. Fulde, and G. Zwicknagl, Phys. Rev. B **69**, 115114 (2004).
[13] V. I. Anisimov, I. A. Nekrasov, D. E. Kondakov, T. M. Rice, and M. Sigrist, Eur. Phys. J. B **25**, 191 (2002).
[14] A. Koga, N. Kawakami, T. M. Rice, and M. Sigrist, Phys. Rev. Lett. **92**, 216402 (2004).
[15] A. Liebsch, cond-mat/0505393 (unpublished).
[16] M. S. Laad, L. Craco, and E. Müller-Hartmann, Europhys. Lett. **69**, 984 (2005).
[17] I. Opahle, S. Elgazzar, K. Koepernik, and P. M. Oppeneer, Phys. Rev. B **70**, 104504 (2004).
[18] R. C. Albers, A. M. Boring, and N. E. Christensen, Phys. Rev. B **33**, 8116 (1986).
[19] D. Sénéchal, D. Perez, and D. Plouffe, Phys. Rev. B **66**, 075129 (2002).
[20] D. Sénéchal, D. Perez, and M. Pioro-Ladriére, Phys. Rev. Lett. **84**, 522 (1999).
[21] D. Sénéchal (unpublished).
[22] Stéphane Pairault, David Sénéchal, and A.-M. S. Tremlay, Eur. Phys. J. B **16**, 85 (2000).
[23] C. Gros and R. Valenti, Ann. Phys. **3**, 460 (1994).
[24] G. Zwicknagl, A. N. Yaresko, and P. Fulde, Phys. Rev. B **65**, 081103(R) (2002).
[25] E. Dagotto, Rev. Mod. Phys. **66**, 763 (1994).
[26] G. L. G. Sleijpen, H. A. V. der Vorst, and Z. Bai (unpublished).
[27] P. Fulde, *Electron Correlations in Molecules and Solids*, 3rd ed. (Springer-Verlag, Berlin, 1995), and references therein.
[28] J. Hubbard, Proc. R. Soc. London, Ser. A **277**, 237 (1963).